JETIR.ORG ISSN: 2349-5162 | ESTD Year : 2014 | Monthly Issue
JOURNAL OF EMERGING TECHNOLOGIES AND INNOVATIVE RESEARCH (JETIR)
An International Scholarly Open Access, Peer-reviewed, Refereed Journal

A High-Voltage Gain Circuit Topology for Minimizing Commutation Torque Ripple with Enhanced Voltage Gain

T.Tharun kumar[1], V.Sunil kumar Reddy[2]
[1]PG Student, Electrical and Electronics Engineering, MJR College Of Engineering & Technology
[2]Associate Professor and HOD, Electrical and Electronics Engineering, MJR College Of Engineering & Technology

Abstract: The electronic commutation and the low inductance nature of the brushless dc motor (BLDC) deteriorate the expected performance. The ripples in the current waveshape are primarily due to the commutation of the phases, which is carried to produce a synchronously rotating magnetic field. This commutation ripples lead to mechanical pulsation and noise on the rotor side. This article presents a novel strategy for reducing the commutation torque ripple. The proposed topology uses a hybrid Cuk voltage ´ gain dc–dc converter at the front end, which has high voltage gain and which reduces voltage ratings of the dc supply. An auxiliary switch is connected across the dc link of the inverter to control the rate of rising incoming phase current during the phase change of the inverter with the help of the dc–dc converter. A prototype of a 1HP BLDC motor is used to validate the proposed topology both analytically and experimentally.

Index Terms: **Brushless dc motor, switched capacitor dc–dc converter, torque ripple compensation**.

I. INTRODUCTION

HE simple design structure and easy control make the brushless dc motor ideal for many applications. Moreover, the low cost, high torque to inertia ratio, reliability, and low maintenance makes it more beneficial in the long run. The constant torque nature of the BLDC motor with trapezoidal back EMF makes it viable for various household and industrial applications [1]–[4]. However, due to practical constraints of the drive, this BLDC machine deviates from the expected constant torque characteristics. This deviation may be due to the imperfect EMF waveform, ripple in the power supply, and the discontinuity produced during the phase current commutation [5]. Rotor skewing is widely implemented for a sinusoidal back EMF type BLDC machine [6]–[8]. The trapezoidal back emf is greatly affected by the winding distribution across the stator. A deviation from the ideal trapezoidal back EMF waveshape could induce more torque ripple in the motor. Even though skewing could affect the trapezoidal waveshape, it will reduce the cogging torque. Hence, in some cases skewing by one stator slot tooth is implemented in the motor design [9]. However, there is a tradeoff between the manufacturing tolerance and cost while we attempt to change the design of the machine to achieve the ideal characteristics. The distortion in current during the commutation interval is one of the major contributor to torque ripple and this drawback cannot be limited by machine design. Ideally a BLDC motor drive is expected to provide rectangular current wave shape in phase with the trapezoidal back EMF by controlling the switching of inverter connected to the stator of the BLDC motor. But the non-ideal nature of the power converter and inductance of the stator winding makes the current to deviate from the rectangular wave shape, which in turn increases the torque ripple. The ripple in torque during such non-ideal situations may be as high as 50% of the electromagnetic torque [5]. This ripple in torque can be minimized by topological modification or by modifying the drive control strategy. The modification in PWM techniques is one of the simplest control technique, which has been widely adopted to improve the torque profile during both commutation period and noncommutation periods [10]. PWM schemes are used for controlling the voltage across the stator phase winding of the motor. The commonly implemented methods are H_PWM_LOW_ON, H_ON_LOW_PWM,PWM_ON_PWM, PWM_PWM, PWM_ON, and ON_PWM [11]–[17]. Most of them have high switching frequency. Some of the issues with high switching frequency is that it may induce a ringing effect between inverter and motor common-mode voltage [18], [19]. In addition, especially for the high power motor drives, the high frequency switching will deteriorate the efficiency of the drive [20], [21]. Another approach adopted for torque ripple reduction is the d-q frame transformation control [22], [23]. This method helps to achieve significant reduction in torque ripple for nonsinusoidal machines by vectorial control. An instantaneous electromagnetic torque calculation during the commutation period from the product of the phase currents and the back EMF is proposed in [24]. Here, the back EMF is calculated using the feedback obtained from the position sensors. This torque estimation is dependent on the values of motor parameters, which is largely affected by the variations in the phase inductance and dc-link voltage. Topological modification of the BLDC drive, which aims at controlling the dc-link voltage for suppression of torque ripple is one of the commonly investigated technique. Most of these topologies provide a higher dc-link voltage during commutation [25]–[30]. In these topologies, dc–dc converter is used to provide the required dc link voltage during the commutation period to adjust

the rise time of the incoming phase current. The immediate transition of input voltage across the dc link is realized with an auxiliary switch [25] connecting the dc link and the output of dc–dc converter.

In [26], a super-lift Luo converter is implemented for obtaining varying voltage across the dc link. This method is implemented on a sinusoidal type back EMF BLDC machine. Therefore, a conspicuous torque ripple reduction was not observed. A Z-source inverter-based torque ripple reduction control is proposed in [27]. The reduction in commutation torque was realized by adjusting the duty cycle. An input voltage control based on optimization technique is presented in [28]. A neural network-based estimation is opted for calculation of the required commutation time and dc-link voltage. The values are optimized using the particle swarm method to minimize the error between the provided reference and actual torque. A diode-assisted buck–boost converter-based topology is proposed in [29]. A diode-based capacitor network is introduced for fast charging of the capacitor to adjust the dc-link voltage at a faster rate. During high-speed conditions or if a disturbance has occurred, there is a possibility of miss conduction of switches of the inverter or shoot through conduction which may impair the inverter.

Hence, it is required to provide a dead time in the switching, which could further extend the commutation time causing an increase in commutation torque ripple [31]. In [30], a reverse blocking IGBT-based novel inverter topology is implemented for controlling the freewheeling current in the BLDC motor. The basic idea of the topology is to provide a higher dc-link voltage through a double layer C-Dump converter during the freewheeling period of the phase current. Also, in [30], the effects of the sensorless control of the BLDC motor are pointed out. A major issue is the false detection of zero crossing of the back EMF resulting in longer commutation period, which may increase the torque ripple. In [32], a novel topology withCuk converter is proposed. This topology operates ´ under two different modes for the BLDC drive. During the normal conduction period, the converter operates in buck–boost mode, and during the commutation period, the converter acts as a boost converter. The modes are controlled by an auxiliary switch based on the feedback signal from the Hall sensor to minimize the torque ripple. This article applies a hybrid Cuk converter-based circuit ´ topology presented in [33] and [34] to a BLDC inverter drive system. The dc-link voltage of the inverter is boosted during the commutation interval. During noncommutation interval, the dc-link voltage appears to be higher than the input dc supply due to the circuit configuration, which in turn helps in reducing the voltage rating of the dc supply. The proposed system effectively improves the performance of the drive by reducing the torque ripple and improving the shape of stator currents. The detailed analysis of the proposed topology is presented in the following sections.

II. SAMPLING AND SYSTEM MODELLING

The equivalent circuit for a three-phase inverter-driven BLDC motor is shown in Fig. 1. The general configuration of a BLDC drive consists of an inverter, a dc source, and a permanent magnet BLDC motor.

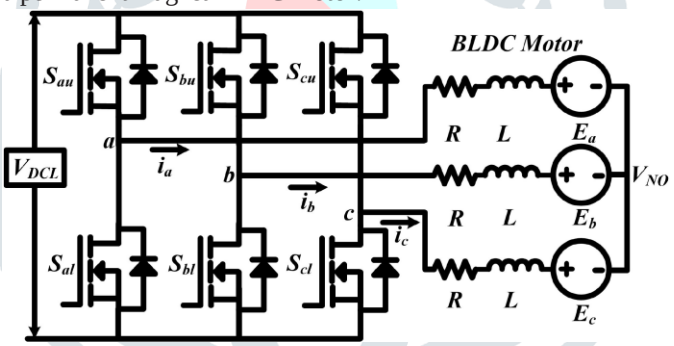

Fig. 1. Equivalent circuit for a three-phase inverter-driven BLDC motor.

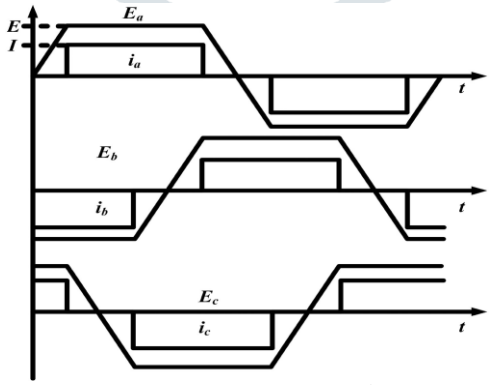

Fig. 2. Back EMF and current waveshape for BLDC drive.

where V_a, V_b, and V_c are the phase voltages. The BLDC motor having symmetrical three-phase winding, consist of equivalent resistance R, inductance L, and line to neutral back EMF E_a, E_b, and E_c. i_a, i_b, and i_c are the phase currents. V_{NO} is the neutral voltage. The instantaneous electromagnetic torque equation may be written as.

where ω_m is the angular rotational speed of the BLDC motor in radians per second.

Fig. 2 shows the ideal waveforms of phase back EMF and phase current for a BLDC motor. V_{DCL} is the dc-link voltage of the two level inverter. It may be observed from Fig. 2 that during noncommutation period only two phases are active. This is shown in the equivalent circuit diagram (see Fig. 3). At a particular instant of time when $E_a = -E_b = -E_c = E$, the current will flow through phase winding a and c as depicted in Fig. 3.

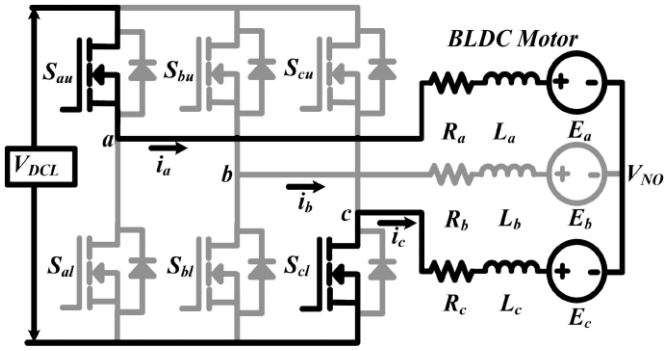

Fig. 3. Phase ac conduction of BLDC drive

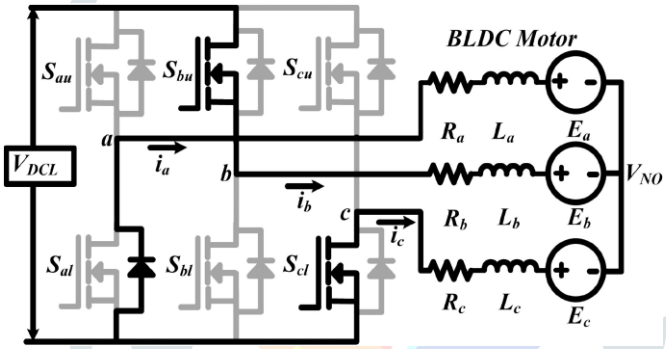

Fig. 4. Phase ABC conduction of BLDC drive.

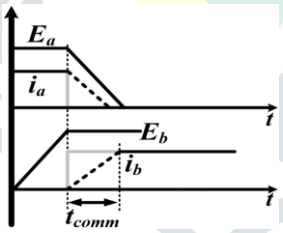

Fig. 5. Phase current during commutation from phase *a* to phase *b*.

The next phase of conduction is in phase *b* and phase *c*. When S_{au} is turned OFF and S_{bu} is turned ON the phase *c* continuous to be in conduction but the current commutes from phase *a* to phase *b*. At this instant, the energy stored in the inductance of phase *a* will freewheel through the body diode of lower switch S_{al} as shown Figs. 4 and 5. The next phase of conduction is in phase *b* and phase *c*. When S_{au} is turned OFF and S_{bu} is turned ON the phase *c* continuous to be in conduction but the current commutes from phase *a* to phase *b*. At this instant, the energy stored in the inductance of phase *a* will freewheel through the body diode of lower switch S_{al} as shown Figs. 4 and 5.

where T_{fall} is the time taken by the phase current i_a to fall from steady-state current *I* to zero, and T_{rise} is the time taken by the current i_b to rise from zero to *I*. The rise time and fall time of the phase current significantly affect the electromagnetic torque ripple of the BLDC motor.

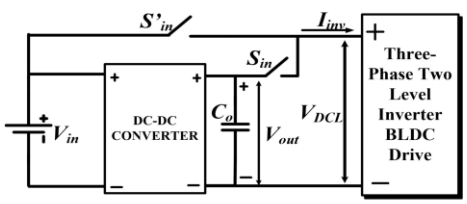

(a)

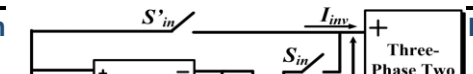

fig. 6. Block Diagram for dc–dc converter based BLDC Drive. (a) Conven- tional Topology. (b) Proposed Topology.

III. PROPOSED TOPOLOGY

The proposed topology uses a hybrid Ćuk voltage gain dc–dc converter at the front end, which has high voltage gain and which reduces voltage ratings of the dc supply. An auxiliary switch is connected across the dc link of the inverter to control the rate of rising incoming phase current during the phase change of the inverter with the help of the dc–dc converter. The circuit topology to minimize the torque ripple of BLDC drive as suggested by [25], [28], [29] is shown in Fig. 6(a). In this configuration, the dc–dc converter connected to the dc link of the inverter through an auxiliary switch Sin and the switch is turned ON during the commutation interval in order to boost the dc-link voltage. Another switch S———————— in is connected in series with the dc source, which is operated in complementary to Sin. An uncontrolled switch (diode) may be used as S———————— in as when Sin is turned ON a reverse voltage appears across S———————— in. The output voltage of the dc–dc converter Vout is made equal to four times the maximum amplitude of the back EMF (4E) to achieve the torque ripple reduction. As the back EMF E depends on speed, the output voltage of dc–dc converter has to vary in accordance with the variation in speed. Fig. 6(b) shows the proposed circuit topology. The Hybrid Cuk converter [33] is used as dc–dc converter in the proposed ´ topology. During the noncommutation period, the capacitor VC and dc-link capacitor Co are connected in series to the input dc supply Vin. This helps in reducing the voltage rating of the dc supply. Detailed analysis is presented in the following section.

Hybrid Cuk DC–DC Converter ´ Fig. 7 shows the Hybrid Cuk dc–dc converter topology. The ´ capacitor network is shown in dotted box helps in increase the voltage gain. The equivalent circuit during the turning ON and OFF of the switch SM are shown in Figs. 8 and 9, respectively. Applying volt-second principle during the ON and OFF time in Figs. 8 and 9 on the inductor Lin and Lo, and the voltage gain.

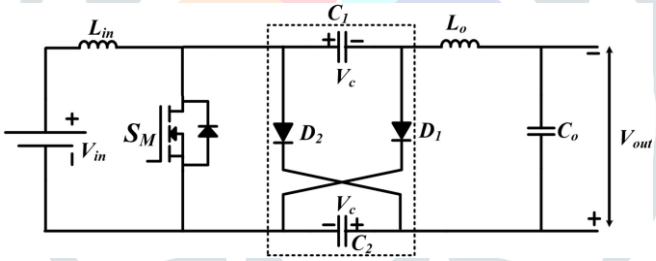

Fig. 7. Implemented dc–dc converter.

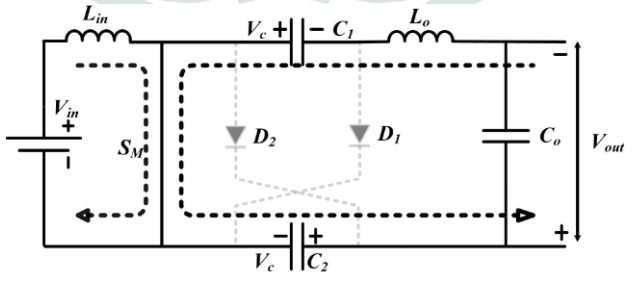

(a)

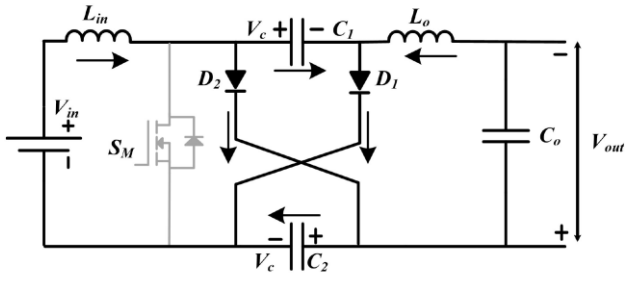

(b)

Fig. 8. Equivalent circuit of the Hybrid Cuk Converter. (a) ´ SM is ON. (b) SM is OFF.

equation is obtained as Vout = (1 + D) (1 − D) Vin. (14) From this, it is apparent that this converter has (1+D) times higher dc voltage gain in comparison to the conventional CUK converter [35]. The equation of voltage across the capacitors C1 and C2 are same as follows: VC = Vin (1 − D) . (15) B. Control Strategy to Reduced Commutation Ripple Fig. 9 shows the circuit topology for the torque ripple reduction. As we know, the dc-link voltage during commutation should be equal to 4E. This voltage is maintained at output of the dc–dc converter by adjusting the duty cycle of switch SM. The switch Sin connects the output of the dc–dc converter to the dc link during the commutation. The back EMF E of the BLDC

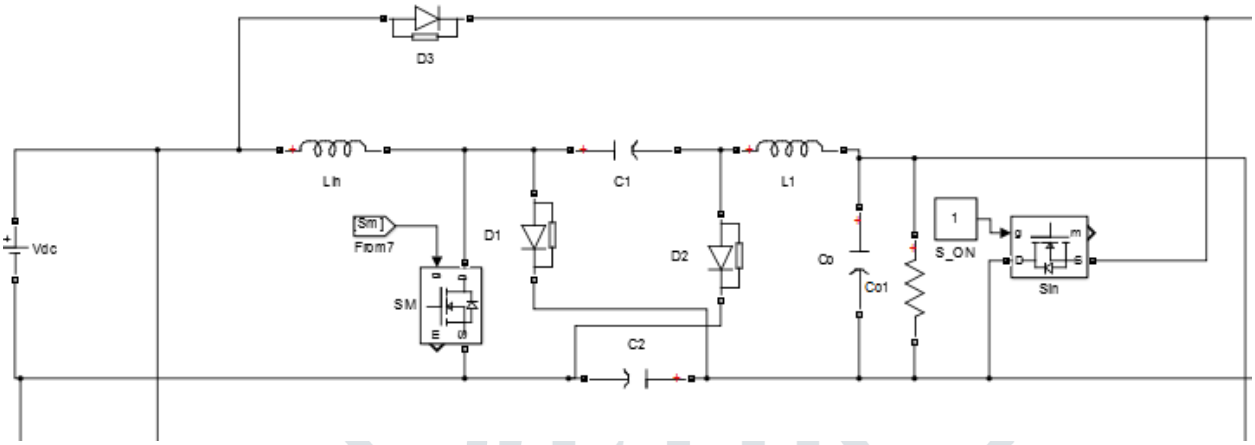

Fig. 9. CUK converter circuit topology.

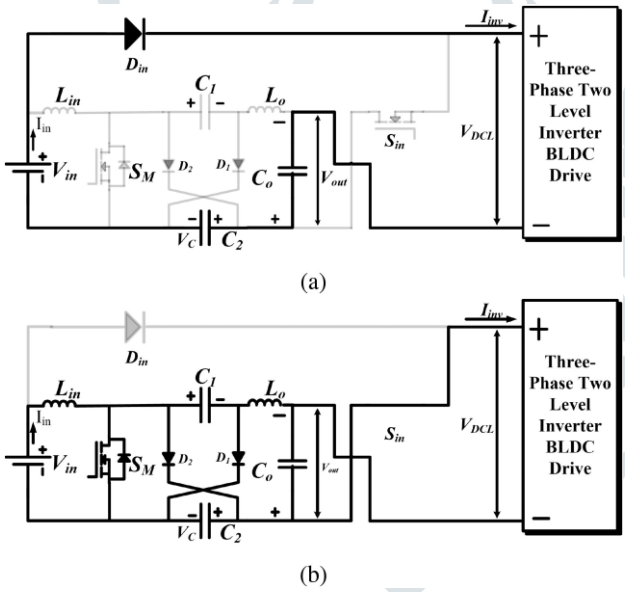

Fig. 10. Conduction Path when (a) S_{in} is OFF (b) S_{in} is ON.

motor is directly proportional to speed, and it is given as E = Keωm (16) where Ke is the back EMF constant. The duty cycle ratio D for switch SM is varied accordingly to reduce the commutation torque ripple. The equation of duty cycle may be calculated as VDCL = 4E (17) D = 4Keωm − VDCL VDCL + 4Keωm . (18) The BLDC motor has six commutation incidents in one electrical cycle. As shown in Fig. 10(b), the switch Sin is turned ON at the start of each commutation incident and turned OFF by calculating the fall time Tfall from (10). The duty ratio D estimated from (18) is applied to the switch SM.

IV. SIMULATION RESULTS:

The proposed BLDC drive was simulated in MAT- LAB/Simulink. The designed parameters of the circuit topology are shown in Table I.The design of the hybrid Ć uk dc–dc converter was validatedusing a MATLAB/Simulink model. A change in duty cycle from 20% to 30% was applied across the converter. It can be observed from Fig. 12 that the time taken for the step change in the output voltage of the

converter is less than 1 ms. At a given low speed of 75 r/min, the conduction period, i.e., the period for which any given phase conducts in the positive or negative half cycle for the given BLDC motor, is less the 67 ms. As the speed increases the time of conduction period decreases. At rated speed of 4000 r/min, the conduction period of the phase is approximately equal to 3.75 ms. The commutation period is much less than the conduction period. It can be estimated from the rise and fall time equations (10) and (11). The commutation period also decreases with increase in speed. During the low speed operation, the dc–dc converter may be used during the transient period of the change in speed. But for the high speed operation, the converter maintain a constant voltage at the dc link during the transient period.

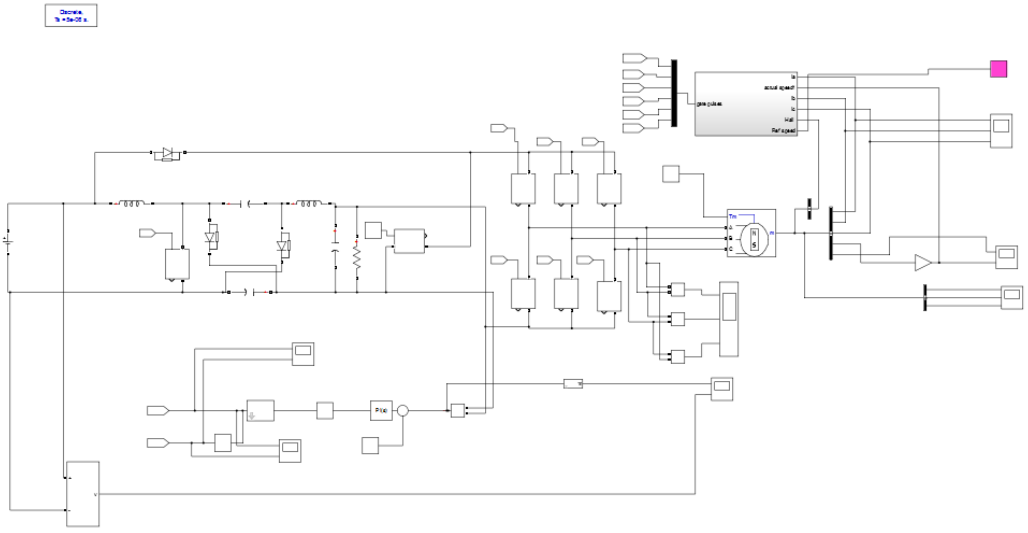

SIMU LINK

However, the hybrid Cuk converter ´ is having faster response in comparison to other converters used in such schemes as shown in [25] and [27]. The proposed circuit topology needs a lower dc supply voltage (V in) to operate the drive at rated supply voltage. To operate the BLDC drive system in the full speed range, the capacitor-assisted dc supply voltage is set to 90 V, generating the required dc voltage during the commutation instant and noncommutation instant for the entire speed range. The conventional PWMON [38] method is used to regulate the speed of the BLDC motor. Fig. 13(a) and (b) shows the simulation result of the BLDC motor operating at rated voltage with an applied load torque of 1.2 N·m. From the simulation result of the BLDC motor, it is apparent that the electromagnetic torque ripple without any compensation for a BLDC motor is very high. The torque ripple generated is approximately equal to 1 N·m, which approximately around 66% of the load torque. The corresponding stator current waveform may be observed in Fig. 13(a). Fig. 14(a), (b), and (c) shows the simulation result for the proposed circuit topology.

A 90 V dc supply voltage V in is applied. A load torque of 1.2 N·m is connected to the motor. The applied dc supply voltage is boosted to the required voltage by adjusting the duty ratio of the dc–dc converter. Fig. 14(b) shows the electromagnetic torque ripple of the proposed topology. The dc link voltage is shown in Fig. 14(c). It may be observed that the phase current waveform is smoother, and the ripples are minimized. The experimental prototype setup of the proposed circuit topology is shown in Fig. 15. An IGBT-based three-phase inverter power module is used. The sensing of current and voltage is done with the help of hall sensors, and the speed is established using feedback hall sensors connected inside the stator of the motor. Code composer studio IDE is used to implement the algorithm to the TMS320F28335 controller board.

A mechanical drum load setup is connected to the shaft of the motor to control the load torque. Fig. 16 shows the experimental result of the uncompenssated motor drive. The ripple in the output current is apparent, which may cause significant mechanical vibrations in the rotor shaft. In order to compare the outcomes of the proposed circuit topology with the uncompensated drive, the motor drive was operated at various conditions. Fig. 17 shows the current and torque responses of the BLDC motor without compensation for three different operating speeds which are in the low, medium, and high speed ranges of the motor. It may be observed that the torque of the motor has significant ripple in all the speed ranges. Figs. 18 and 19 show the phase current, torque, and speed responses for the BLDC motor with the proposed circuit topology for the same operating conditions as in Fig. 17. It is clear from the responses that the current waveshape is nearly ideal, and the torque ripple is reduced for all the operating speed.

INPUT VOLTAGE

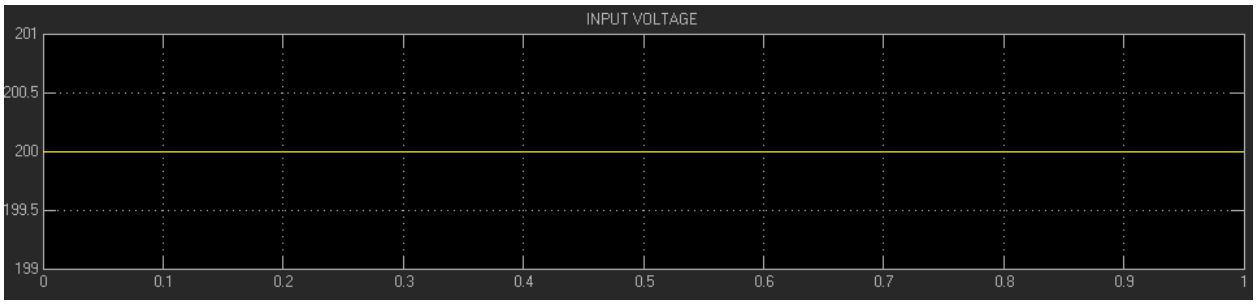

CONVERTER VOLTAGE

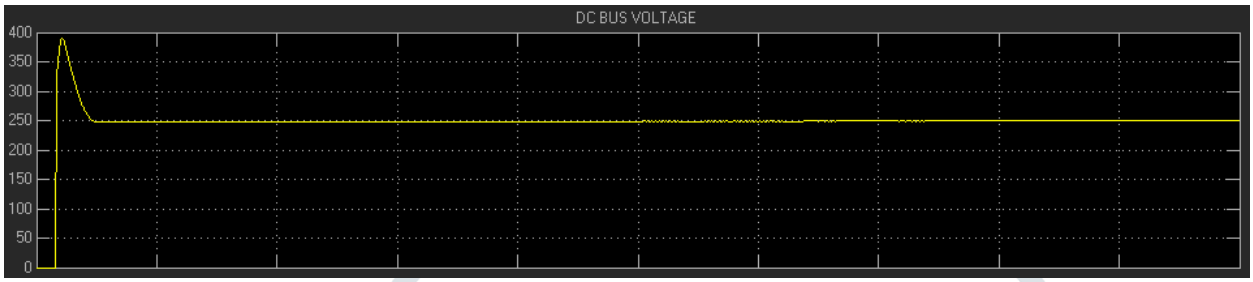

3 PHASE INVERTER VOLTAGE

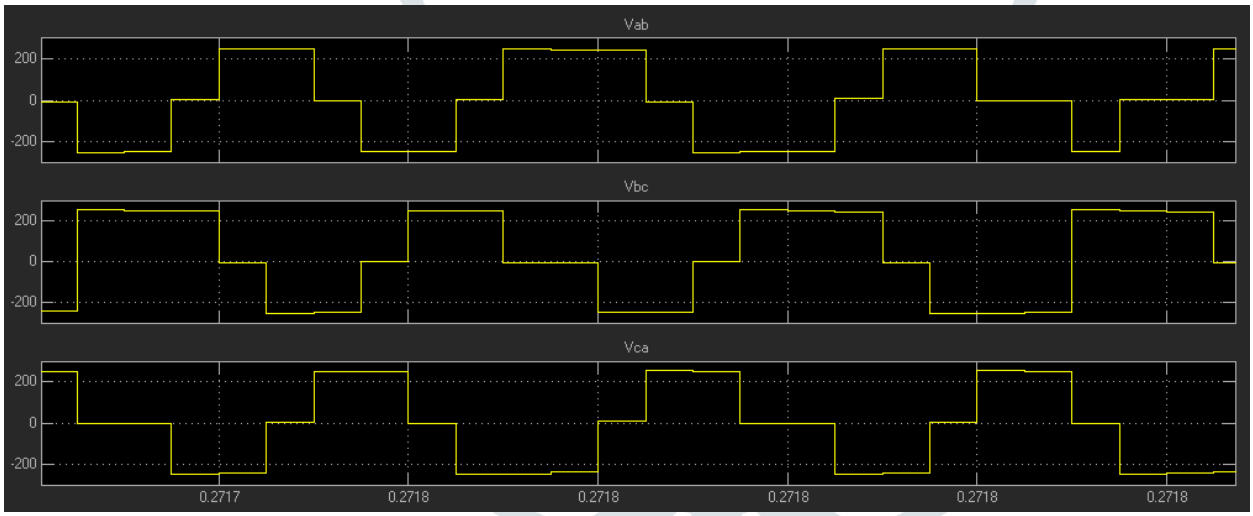

MOTOR CURRENT

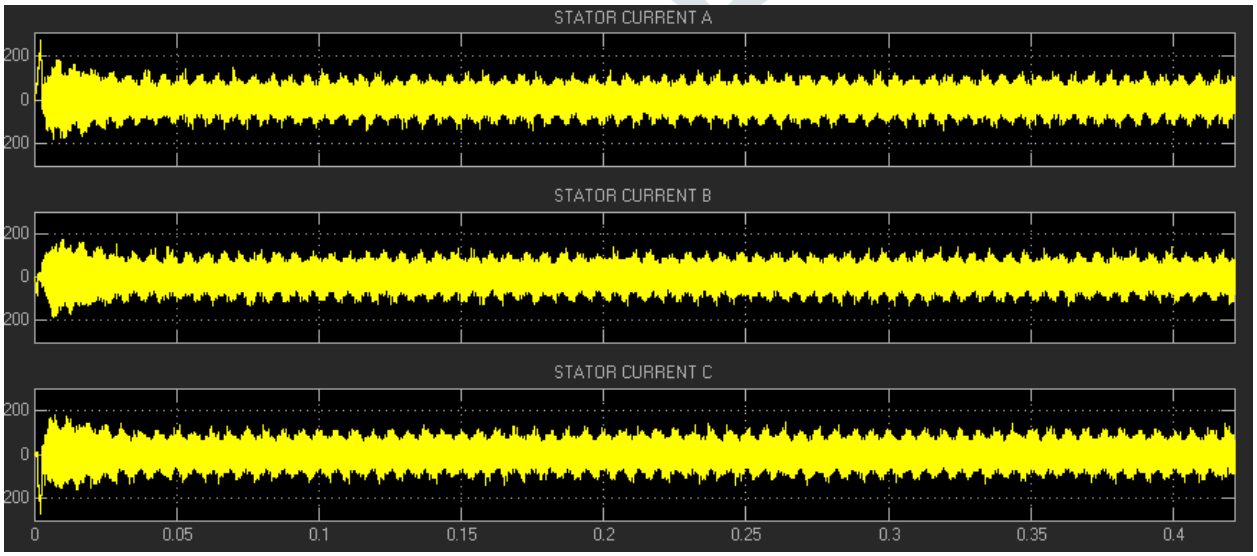

MOTOR SPEED

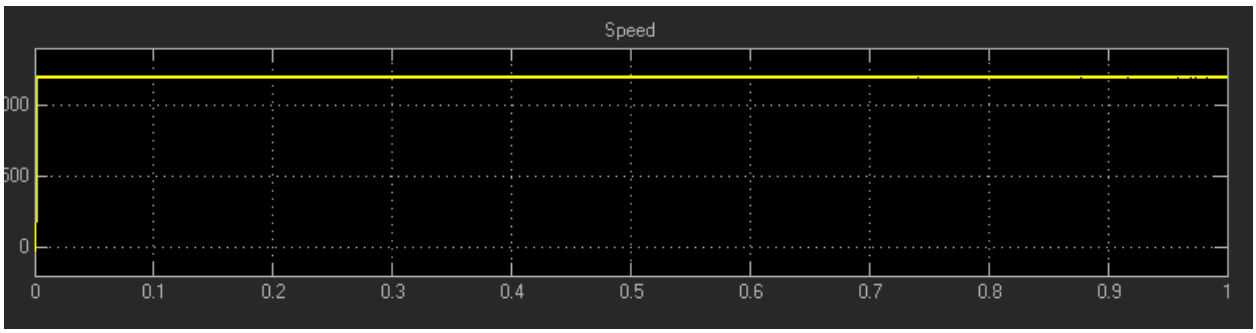

BACK EMF

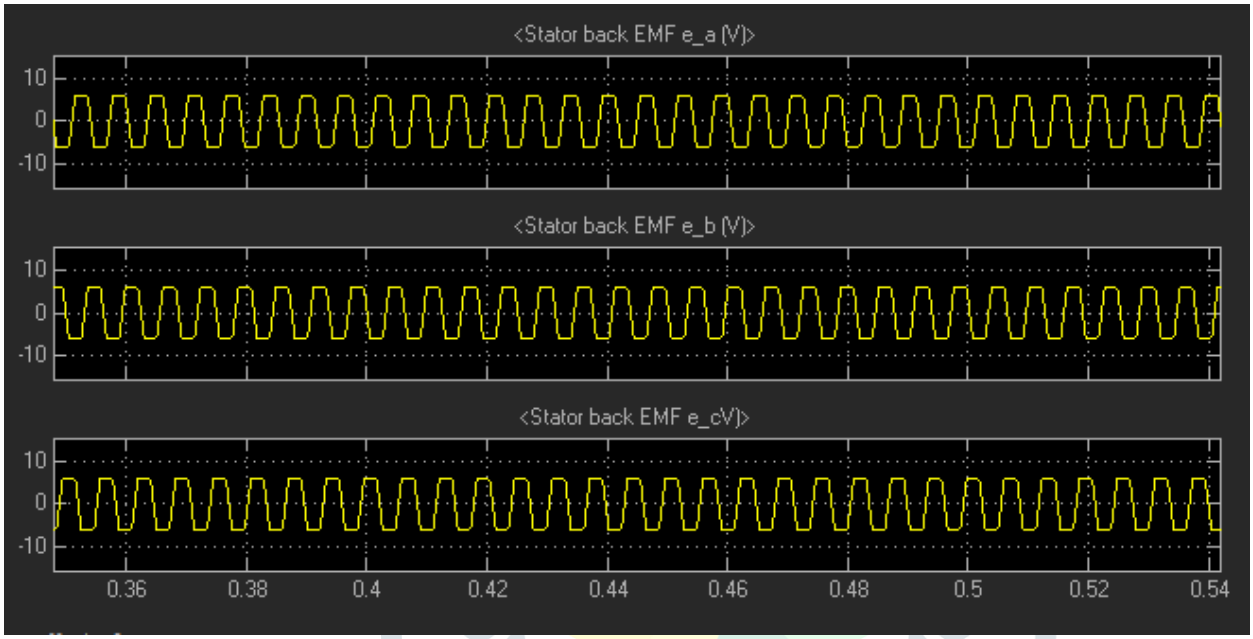

V. CONCLUSION

The proposed circuit topology significantly improves the performance of the BLDC drive. From the results, it can be concluded that the proposed method is reliable and efficient. The proposed circuit topology puts forward some distinct advantages over the earlier studied topologies for torque ripple suppression, which can be enumerated as follows: 1) The drive requires a lower input supply voltage to operate the motor at rated conditions. 2) The high gain Hybrid Cuk dc–dc converter requires a ´ lesser size of magnetic elements, which reduces the weight of the drive system. 3) The implemented high gain converter will reduce the stress on the converter switch since extreme duty cycle operation will not be required because of the higher boosting ratio This proposed converter topology will be advantageous for the drive system where the motor's rated voltage is higher than the available dc supply voltage. The proposed circuit topology significantly improves the performance of the BLDC drive. The future scope of this work is very wide. Extending this study to the above rated speed conditions through flux weakening by operating the inverter with pulse amplitude modulation will be a very interesting addition to this work.

VI. REFERENCES

[1] Z. Q. Zhu and J. H. Leong, "Analysis and mitigation of torsional vibration of PM brushless AC/DC drives with direct torque controller," IEEE Trans. Ind. Appl., vol. 48, no. 4, pp. 1296–1306, Jul./Aug. 2012.

[2] Y.-C. Son, K. Y. Jang, and B.-S. Suh, "Integrated MOSFET inverter module for low-power drive system," IEEE Trans. Ind. Appl., vol. 44, no. 3, pp. 878–886, May/Jun. 2008.

[3] R. Islam, I. Husain, A. Fardoun, and K. McLaughlin, "Permanent-magnet synchronous motor magnet designs with skewing for torque ripple and cogging torque reduction," IEEE Trans. Ind. Appl., vol. 45, no. 1, pp. 152–160, Jan./Feb. 2009.

[4] B. Akin, M. Bhardwaj, and J. Warriner, "Trapezoidal control of BLDC motors using hall effect sensors," Texas Instruments, Dallas, TX, USA, 2010.

[5] R. Carlson, M. Lajoie-Mazenc, and J. Fagundes, "Analysis of torque ripple due to phase commutation in brushless DC machines," IEEE Trans. Ind. Appl., vol. 28, no. 3, pp. 632–638, May/Jun. 1992.

[6] N. Bianchi and S. Bolognani, "Design techniques for reducing the cogging torque in surface-mounted PM motors," IEEE Trans. Ind. Appl., vol. 38, no. 5, pp. 1259–1265, Sep./Oct. 2002.

[7] Z. S. Du and T. A. Lipo, "Efficient utilization of rare earth permanentmagnet materials and torque ripple reduction in interior permanentmagnet machines," IEEE Trans. Ind. Appl., vol. 53, no. 4, pp. 3485–3495, Jul./Aug. 2017.

[8] M. Islam, S. Mir, and T. Sebastian, "Issues in reducing the cogging torque of mass-produced permanent-magnet brushless DC motor," IEEE Trans. Ind. Appl., vol. 40, no. 3, pp. 813–820, May./Jun. 2004.

[9] T. Sebastian and V. Gangla, "Analysis of induced EMF waveforms and torque ripple in a brushless permanent magnet machine," IEEE Trans. Ind. Appl., vol. 32, no. 1, pp. 195–200, Jan./Feb. 1996.

[10] J. Shi and T.-C. Li, "New method to eliminate commutation torque ripple of brushless DC motor with minimum commutation time," IEEE Trans. Ind. Electron., vol. 60, no. 6, pp. 2139–2146, Jun. 2013.

[11] Y.-K. Lin and Y.-S. Lai, "Pulsewidth modulation technique for BLDCM drives to reduce commutation torque ripple without calculation of commutation time," IEEE Trans. Ind. Appl., vol. 47, no. 4, pp. 1786–1793, Jul./Aug. 2011.

[12] J. Shao, D. Nolan, M. Teissier, and D. Swanson, "A novel microcontrollerbased sensorless brushless DC (BLDC) motor drive for automotive fuel pumps," IEEE Trans. Ind. Appl., vol. 39, no. 6, pp. 1734–1740, Nov./Dec. 2003.

[13] Y.-S. Lai, F.-S. Shyu, and Y.-K. Lin, "Novel PWM technique without causing reversal dc-link current for brushless DC motor drives with bootstrap driver," in Proc. 40th IAS Annu. Meeting. Conf. Rec. Ind. Appl. Conf., 2005, vol. 3, pp. 2182–2188.

[14] D. Busse, J. Erdman, R. Kerkman, D. Schlegel, and G. Skibinski, "The effects of PWM voltage source inverters on the mechanical performance of rolling bearings," IEEE Trans. Ind. Appl., vol. 33, no. 2, pp. 567–576, Mar./Apr. 1997.

[15] Y.-S. Lai, F.-S. Shyu, and Y.-H. Chang, "Novel loss reduction pulsewidth modulation technique for brushless DC motor drives fed by MOSFET inverter," IEEE Trans. Power Electron., vol. 19, no. 6, pp. 1646–1652, Nov. 2004.

[16] G. Meng, H. Xiong, and H. Li, "Commutation torque ripple reduction in BLDC motor using PWM on PWM mode," in Proc. Int. Conf. Elect. Mach. Syst., 2009, pp. 1–6.

[17] Y.-S. Lai, F.-S. Shyu, and Y.-H. Chang, "Novel pulse-width modulation technique with loss reduction for small power brushless DC motor drives," in Proc. Conf. Rec. IEEE Ind. Appl. Conf. 37th IAS Annu. Meeting (Cat. No.02CH37344), 2002, vol. 3, pp. 2057–2064.

[18] D. Han, C. T. Morris, W. Lee, and B. Sarlioglu, "Comparison between output cm chokes for sic drive operating at 20- and 200-khz switching frequencies," IEEE Trans. Ind. Appl., vol. 53, no. 3, pp. 2178–2188, May/Jun. 2017.

[19] S. Singh, N. B. Y. Gorla, K. Jayaraman, and J. Pou, "Analysis and mitigation of the common-mode noise in a three-phase sic-based brushless DC motor drive with 120◦ conduction mode," IEEE Trans. Power Electron., vol. 37, no. 5, pp. 5514–5523, May 2022.

[20] Y.-S. Lai and Y.-k. Lin, "Assessment of pulse-width modulation techniques for brushless DC motor drives," in Proc. Conf. Rec. IEEE Ind. Appl. Conf. 41st IAS Annu. Meeting, 2006, vol. 4, pp. 1629–1636.

[21] J. Fang, H. Li, and B. Han, "Torque ripple reduction in BLDC torque motor with nonideal back EMF," IEEE Trans. Power Electron., vol. 27, no. 11, pp. 4630–4637, Nov. 2012.

[22] S. J. Park, H. W. Park, M. H. Lee, and F. Harashima, "A new approach for minimum-torque-ripple maximum-efficiency control of BLDC motor," IEEE Trans. Ind. Electron., vol. 47, no. 1, pp. 109–114, Feb. 2000.

[23] A. Vagati, A. Fratta, G. Franceschini, and P. Rosso, "AC motors for highperformance drives: A design-based comparison," IEEE Trans. Ind. Appl., vol. 32, no. 5, pp. 1211–1219, Sep./Oct. 1996.